

Performance evaluation of data-driven techniques for the softwarized and agnostic management of an N×N photonic switch

Original

Performance evaluation of data-driven techniques for the softwarized and agnostic management of an N×N photonic switch / Khan, Ihtesham; Tunesi, Lorenzo; Masood, Muhammad Umar; Ghillino, Enrico; Bardella, Paolo; Carena, Andrea; Curri, Vittorio. - In: OPTICS CONTINUUM. - ISSN 2770-0208. - ELETTRONICO. - 1:1(2022), pp. 1-15. [10.1364/OPTCON.428567]

Availability:

This version is available at: 11583/2950212 since: 2022-01-25T23:37:48Z

Publisher:

Optica Publishing Group

Published

DOI:10.1364/OPTCON.428567

Terms of use:

This article is made available under terms and conditions as specified in the corresponding bibliographic description in the repository

Publisher copyright

Optica Publishing Group (formely OSA) postprint versione editoriale con OAPA (OA Publishing Agreement)

© 2022 Optica Publishing Group. Users may use, reuse, and build upon the article, or use the article for text or data mining, so long as such uses are for non-commercial purposes and appropriate attribution is maintained. All other rights are reserved.

(Article begins on next page)

Strong Exciton Binding in Quantum Structures through Remote Dielectric Confinement

Guido Goldoni, Fausto Rossi, and Elisa Molinari

*Istituto Nazionale per la Fisica della Materia (INFM), and Dipartimento di Fisica, Università di Modena,
Via Campi 213/A, I-41100 Modena, Italy*

(Received 10 February 1998)

We propose a new type of hybrid systems formed by conventional semiconductor nanostructures with the addition of remote insulating layers, where the electron-hole interaction is enhanced by combining *quantum* and *dielectric confinement* over different length scales. Because of the polarization charges induced by the dielectric mismatch at the semiconductor/insulator interfaces, we show that the exciton binding energy can be more than doubled. For conventional III-V quantum wires such remote dielectric confinement allows exciton binding at room temperature. [S0031-9007(98)06255-3]

PACS numbers: 78.66.Fd, 71.35.-y, 73.20.Dx, 77.55.+f

The electron-hole Coulomb interaction in semiconductors leads to bound excitonic states that could play a crucial role in the next generation of optical devices. For this purpose, however, the binding energy E_b must exceed the thermal energy at room temperature, a condition that is not yet met in conventional III-V materials. In fact, a large enhancement of E_b with respect to bulk materials has been obtained by confining electron and hole wave functions in nanostructures of low dimensionality (quantum confinement), the most promising type of structures being quasi-one-dimensional systems (quantum wires); within GaAs-based materials, however, the observed values of E_b are still well below the room-temperature thermal energy.

In this Letter we propose an alternative approach to enhance E_b that combines *quantum confinement* with *remote dielectric confinement*. As first pointed out by Keldysh [1], the electron-hole Coulomb attraction can be greatly enhanced in layered structures with strong dielectric mismatch, due to the polarization charge induced at the interfaces. For conventional semiconductor nanostructures such as GaAs/AlGaAs- or GaAs/InGaAs-based samples, however, this is a minor effect due to the small dielectric mismatch between the constituents [2]. On the other hand, interfaces between III-V semiconductors and materials with very different dielectric constants, such as oxides, are usually very far from the excellent optical quality of the conventional ones. Our approach is based on the idea that *quantum and dielectric confinement can be spatially separated*, since they are effective over different length scales. We will show that a very large increase in E_b can be obtained in GaAs-based quantum wires by adding remote insulating layers: these induce strong dielectric confinement without degrading the good optical properties ensuing from quantum confinement.

We consider GaAs/AlGaAs quantum wires (QWI), where excitonic properties have been studied extensively [3]. We focus on QWIs with T-shaped [4] and V-shaped [5] cross sections, which rank among the best available samples from the point of view of optical properties. Starting from these geometries, we design hybrid struc-

tures adding oxide layers at some distance from the QWI. In the new structures, the electron and hole wave functions are confined by the inner, lattice-and-dielectric-matched GaAs/AlGaAs interfaces; the outer AlGaAs/oxide interfaces, owing to the strong dielectric mismatch, provide polarization charges, thus enhancing the electron-hole interaction.

To obtain quantitative predictions of excitonic properties in such hybrid structures, an accurate description of the complex interplay between quantum and dielectric confinement is needed. To this end, we have developed a novel theoretical scheme that allows us to treat arbitrary dielectric configurations, where the low symmetry makes simple image-charge methods [2,6] not applicable. Furthermore, we adopt a nonperturbative approach for the self-energy term, which, in principle, is needed to describe strong dielectric mismatch combined with shallow confining potentials, as in some state-of-the-art QWIs. The electron-hole interaction is treated within the conventional approach of the semiconductor Bloch equations, adapted to quasi-one-dimensional (1D) systems [7].

More specifically, for a spatially modulated dielectric constant $\epsilon(\mathbf{r})$ the Coulomb interaction between two charges of opposite sign $\pm e$ sitting at positions \mathbf{r} and \mathbf{r}' —our electron-hole pair—is given by $V(\mathbf{r}, \mathbf{r}') = -e^2 G(\mathbf{r}, \mathbf{r}')$, where $G(\mathbf{r}, \mathbf{r}')$ is the Green's function of the Poisson operator, i.e.,

$$\nabla_{\mathbf{r}} \cdot \epsilon(\mathbf{r}) \nabla_{\mathbf{r}} G(\mathbf{r}, \mathbf{r}') = -\delta(\mathbf{r} - \mathbf{r}'). \quad (1)$$

We see that the space dependence of $\epsilon(\mathbf{r})$ modifies $G(\mathbf{r}, \mathbf{r}')$ with respect to the homogeneous case, where $\epsilon(\mathbf{r}) = \epsilon_0$ implies $G_0(\mathbf{r}, \mathbf{r}') = \frac{1}{4\pi\epsilon_0 |\mathbf{r} - \mathbf{r}'|}$. This, in turn, gives rise to significant modifications in the excitonic spectrum; within the conventional Hartree-Fock scheme, such modifications originate from the electron-hole Coulomb matrix elements entering the evaluation of the absorption spectrum [7],

$$V_{ij}^{eh} = -e^2 \int \Phi_i^{e*}(\mathbf{r}) \Phi_j^{h*}(\mathbf{r}') G(\mathbf{r}, \mathbf{r}') \Phi_i^h(\mathbf{r}') \Phi_j^e(\mathbf{r}) d\mathbf{r} d\mathbf{r}'. \quad (2)$$

Here $\Phi_l^{e(h)}$ denotes the electron (hole) single-particle envelope function for the $l \equiv k_z, \nu$ state of the QWI, k_z the wave vector along the wire, and ν the subband index.

To study realistic geometries, we find it convenient to cast the problem in Fourier space, following the theoretical scheme in Ref. [7]. It is easy to rewrite Eqs. (1) and (2) (the symbol $\tilde{}$ denotes Fourier transform throughout):

$$\sum_{\mathbf{k}''} \tilde{\epsilon}(\mathbf{k} - \mathbf{k}'') \mathbf{k} \cdot \mathbf{k}'' \tilde{G}(\mathbf{k}'', \mathbf{k}') = \delta(\mathbf{k} + \mathbf{k}'), \quad (3)$$

$$V_{ij}^{eh} = -e^2 \sum_{\mathbf{k}} F_{ij}^e(\mathbf{k}) \sum_{\mathbf{k}'} \tilde{G}(\mathbf{k}, \mathbf{k}') F_{ji}^h(\mathbf{k}'), \quad (4)$$

where $F_{lm}^{e/h}(\mathbf{k}) = \int \Phi_l^{e/h*}(\mathbf{r}) e^{i\mathbf{k} \cdot \mathbf{r}} \Phi_m^{e/h}(\mathbf{r}) d\mathbf{r}$. We stress that, in order to evaluate the Coulomb matrix elements in (4), it is not necessary to solve Eq. (3) for each $\tilde{G}(\mathbf{k}, \mathbf{k}')$. In fact, if we multiply (3) by $F_{ji}^h(\mathbf{k}')$ and sum over \mathbf{k}' , we get a Poisson equation for the “potential” $v_{ji}(\mathbf{k}) = \sum_{\mathbf{k}'} \tilde{G}(\mathbf{k}, \mathbf{k}') F_{ji}^h(\mathbf{k}')$ [see Eq. (4)] arising from the “source” $F_{ji}^h(\mathbf{k}')$, which is solved only once for each pair i, j .

The Green's function $G(\mathbf{r}, \mathbf{r}')$ also gives rise to a self-energy term

$$\Sigma(\mathbf{r}) = \frac{e^2}{2} \lim_{\mathbf{r}' \rightarrow \mathbf{r}} [G(\mathbf{r}, \mathbf{r}') - G_B(\mathbf{r}, \mathbf{r}')], \quad (5)$$

where $G_B(\mathbf{r}, \mathbf{r}') = \frac{1}{4\pi\epsilon(\mathbf{r})|\mathbf{r} - \mathbf{r}'|}$ is the (local) bulk solution of (1). Σ is a local correction (equal for electrons and holes) which adds to the confining potential in determining the single-particle envelope functions $\Phi_l^{e/h}$. This self-energy contribution is evaluated within the same plane-wave approach by solving (3) at a set of \mathbf{k}' [8]: it can be shown that its Fourier transform is

$$\tilde{\Sigma}(\mathbf{G}) = \frac{e^2}{2} \sum_{\mathbf{g}} \left[\tilde{G}\left(\mathbf{G} + \frac{\mathbf{g}}{2}, \mathbf{G} - \frac{\mathbf{g}}{2}\right) - \tilde{G}_B(\mathbf{G}, \mathbf{g}) \right], \quad (6)$$

where $\tilde{G}_B(\mathbf{G}, \mathbf{g}) = \tilde{\epsilon}^{-1}(\mathbf{G})/g^2$ with the definitions $\mathbf{G} = (\mathbf{k} + \mathbf{k}')/2$ and $\mathbf{g} = \mathbf{k} - \mathbf{k}'$ [9].

We first discuss our findings for QWIs obtained by epitaxial growth on V-grooved substrates (V-QWIs) [5]. As a reference sample, we consider a GaAs wire with AlAs barriers [10], and we add two oxide layers, below and above the QWI [see Fig. 1(a)], at a distance L from the GaAs/AlAs interfaces [11]. Note that the oxide layers are characterized by a small dielectric constant that we take equal to 2 [12].

Our results for the V-QWRs are shown in Fig. 1. For the sample shown in Fig. 1(a), we find $E_b = 29.3$ meV, to be compared with 13 meV of the conventional (i.e., with no oxide layers) structure. Figure 1(a) shows that the origin of this dramatic enhancement is the large polarization of the AlAs/oxide interfaces induced by the hole charge density [13]; the polarization is larger in the region where

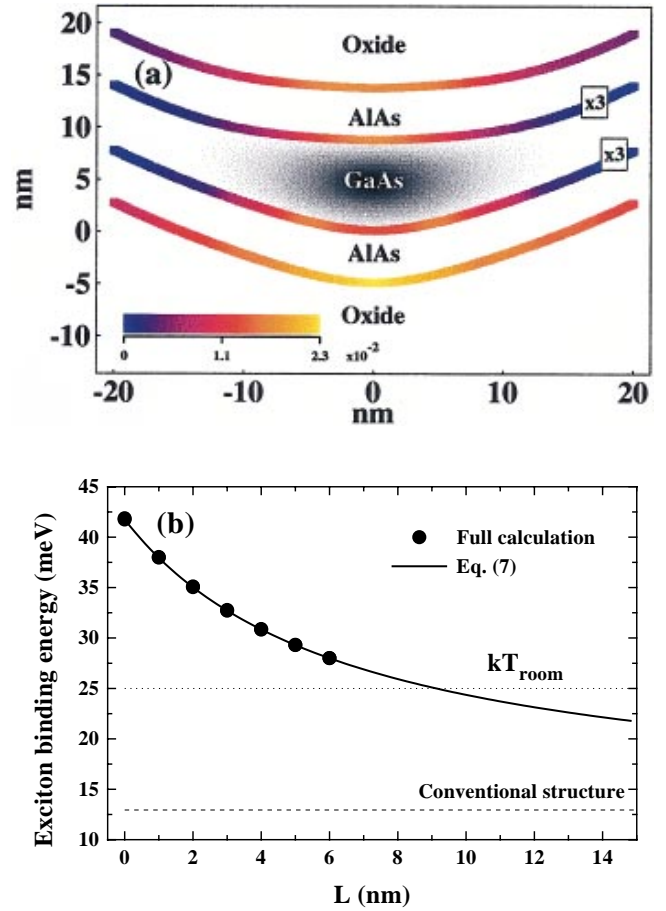


FIG. 1. (a) (color) Cross section of a hybrid V-QWI, showing the interface polarization charge (colors, units of nm^{-1}) induced by the charge-density distribution of the lowest-subband hole (grey scale, arbitrary units). The profile of the GaAs/AlAs interfaces is obtained from Ref. [10]; the oxide layers are at $L = 5$ nm from the GaAs/AlAs interfaces. The polarization charge at the GaAs/AlAs interfaces is multiplied by 3. (b) E_b versus distance of the oxide layers from the internal interfaces, L . Solid dots: Full calculation. Solid line: Eq. (7) with $L_0 = 6.56$ nm. Dashed line: Energy E_0 of the corresponding conventional structure (no oxide layers). Dotted line: thermal energy at $T_{\text{room}} = 300$ K.

the hole is localized, and is more pronounced at the lower interface, due to the larger curvature. A small polarization charge is also induced at the GaAs/AlAs interface, due to the small dielectric mismatch. Note that quantum confinement localizes the wave function well within the inner interfaces; therefore, the AlAs/oxide interface does not affect the electron and hole wave functions.

In Fig. 1(b) we show the calculated E_b for selected values of L . We also show, for comparison, the calculated binding energy for the conventional structure, E_0 , and the room-temperature thermal energy. E_b is maximum when the oxide layer is at minimum distance [14], $L = 0$: it is enhanced by a factor larger than 3 with respect to E_0 , and it is well above kT_{room} [15]. It is important to note that E_b decreases slowly with L , and is still significantly

larger than kT_{room} at $L = 6$ nm. Since E_b is the result of the Coulomb interaction of, say, the electron with the hole *and* the polarization charge which is excited at a distance $\sim L$, we intuitively expect E_b to decay as L^{-1} , with a typical decay length L_0 comparable to the Bohr radius in the QWI [7]; this, in turn, is of the order of the confinement length. Indeed, Fig. 1(b) shows that E_b is very well interpolated by

$$E_b(L) = E_0 + \frac{E_b(0)}{1 + L/L_0}, \quad (7)$$

with $L_0 = 6.56$ nm. Note that E_b crosses kT_{room} when L is as large as 9 nm.

A second type of structures, which have recently attracted considerable attention, are the so-called T-shaped wires (T-QWI), obtained by the cleaved-edge overgrowth method [3,4]. The typical sample of our calculations [see Fig. 2(a)] consists of a T-QWI with GaAs parent quantum wells (QWs) of the same width, and AlAs barriers. An

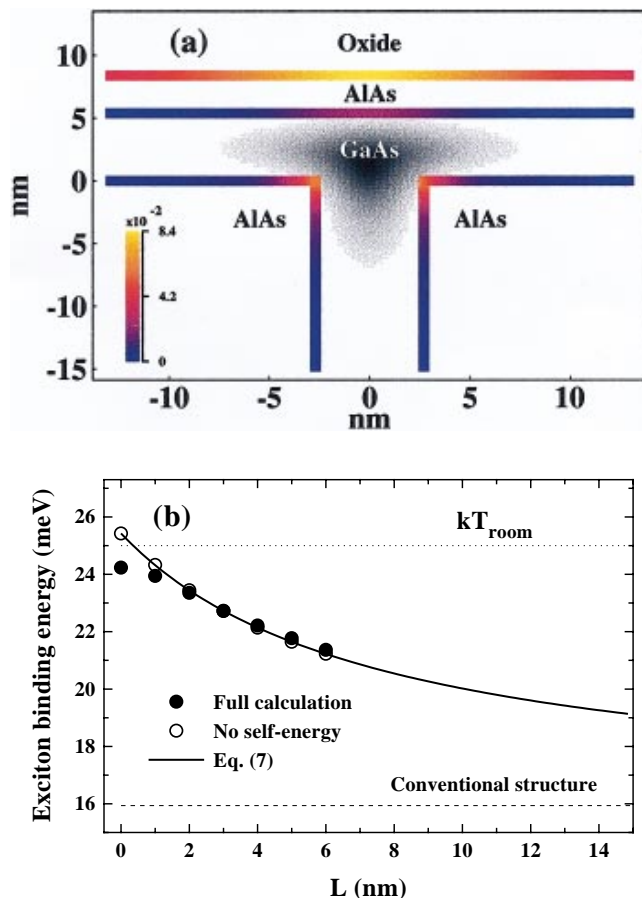


FIG. 2. (a) (color) Same as Fig. 1(a) for a hybrid T-QWI. The QW widths are 5.4 nm; the oxide layer is at $L = 3$ nm from the GaAs/AlAs interface. (b) E_b versus L including (solid dots) and neglecting (empty dots) the self-energy contribution. Solid line: Eq. (7) with $L_0 = 7.55$ nm. Dashed line: Energy E_0 of the corresponding conventional structure (no oxide layers). Dotted line: Thermal energy at $T_{\text{room}} = 300$ K.

oxide layer is added on top of the exposed surface at a distance L from the underlying QW. Note that, in this case, an oxide layer is present only on one side of the QWI. As in the case of the V-QWIs, a strong polarization charge forms at the AlAs/oxide interface, with a maximum in the region of the hole wave function confinement. A small polarization charge is also present at the GaAs/AlAs interface, peaked around the corners of the intersecting QWs. In Fig. 2(b) we show the calculated E_b vs L . The binding energy for the conventional structure, E_0 , and the room-temperature thermal energy are also shown for comparison. As in the case of the V-QWI, E_b is maximum at $L = 0$, where it is enhanced by a factor of 1.5 with respect to E_0 , and decreases slowly with L . Although E_b is smaller than in the case of the V-QWI studied previously, for the smallest L values E_b is still of the order of kT_{room} . It is important to note that the reduced effect of dielectric confinement in the T-QWI sample with respect to the previous example of V-QWI is just due to the presence of a single oxide layer; i.e., geometric effects due to different cross sections play a minor role. In fact, despite the very different geometry, E_b decays with L in the same way in both cases. As shown in Fig. 2(b), also in the case of T-QWIs E_b is very well interpolated by Eq. (7) with $L_0 = 7.55$ meV, which is still of the order of the QWI confinement length. Note that the above examples of structures are based on standard state-of-the-art QWIs that were previously studied in the literature [4,5], and no particular optimization of E_b with respect to sample parameters (constituents and/or geometry) has been attempted.

Finally, we discuss the effect of the self-energy term on E_b . We have compared the full calculations discussed above with calculations performed neglecting $\Sigma(\mathbf{r})$ in the single-particle potential. For the V-QWI we have verified that the self-energy contribution tends to increase E_b , but it is so small (<0.2 meV) that the two results cannot be distinguished on the scale of Fig. 1(b). In the case of the T-QWIs, on the other hand, the self-energy contribution is qualitatively and quantitatively different, as can be seen from Fig. 2(b); in this case, in fact, it amounts to ~ 1 meV at the smallest L , and tends to reduce E_b . This is a consequence of the interplay between the dielectric confinement and the shallow quantum confinement of these structures; this is apparent from Fig. 3, where we compare the electron and hole single-particle wave functions calculated neglecting [Fig. 3(a)] and including [Fig. 3(b)] the self-energy term. The self-energy potential [Fig. 3(c)] inside the GaAs layer pushes the electron and hole wave functions away from the oxide layer; because of the different masses and shallow confining potentials, such shift is different for electrons and holes, and the overlap is diminished, thereby reducing E_b .

In summary, we have developed a theoretical scheme that allows us to include dielectric confinement and self-energy effects in a full three-dimensional description of correlated electron-hole pairs [16]. Our calculations

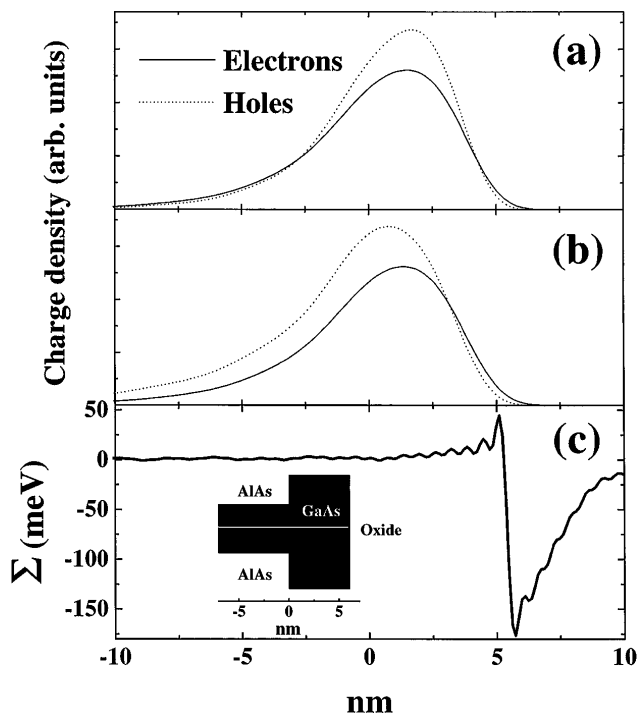


FIG. 3. Lowest-subband electron and hole charge densities for a T-QWI with $L = 0$ (see inset), neglecting (a) and including (b) the self-energy potential $\Sigma(\mathbf{r})$ shown in (c). All curves are calculated along the white line shown in the inset.

show that a dramatic enhancement of the exciton binding in GaAs-based quantum structures is made possible by remote insulating layers, bringing E_b in the range of the room-temperature thermal energy. This enhancement scales slowly with the distance of the insulating layer from the quantum confinement region, thus allowing one to design nanostructures that should be compatible with excellent optical efficiency. Dielectric confinement by remote insulating layers is predicted to be a novel powerful tool for tailoring excitonic confinement in semiconductor nanostructures.

We are grateful to E. Kapon, L. Sorba, and W. Wegscheider for useful discussions. This work was supported in part by the EC through the TMR Network *Ultrafast quantum optoelectronics*.

- [1] L. V. Keldysh, Pis'ma Zh. Eksp. Teor. Fiz. **29**, 716 (1979) [JETP Lett. **29**, 658 (1979)].
- [2] L. C. Andreani and A. Pasquarello, Phys. Rev. B **42**, 8928 (1990).
- [3] For recent reviews see H. Sakaki *et al.*, in *Proceedings of the Fifth International Meeting on Optics of Excitons in Confined Systems* [Phys. Status Solidi (a) **164**, 241

(1997)]; G. Goldoni, F. Rossi, and E. Molinari, *ibid.* **164**, 265 (1997).

- [4] L. Pfeiffer *et al.*, Appl. Phys. Lett. **56**, 1697 (1990).
- [5] E. Kapon *et al.*, Phys. Rev. Lett. **63**, 430 (1989).
- [6] M. Kumagai and T. Takagahara, Phys. Rev. B **40**, 12359 (1989).
- [7] F. Rossi and E. Molinari, Phys. Rev. Lett. **76**, 3642 (1996); Phys. Rev. B **53**, 16462 (1996); F. Rossi, G. Goldoni, and E. Molinari, Phys. Rev. Lett. **78**, 3527 (1997).
- [8] It turns out that $\tilde{G}(\mathbf{k}, \mathbf{k}')$ is needed on a coarser grid for \mathbf{k}' than for \mathbf{k} , due to the different length scales of quantum and dielectric confinements; this makes the numerical evaluation of (6) feasible.
- [9] To avoid numerical instabilities we found it convenient to define a reference material with the homogeneous dielectric constant $\epsilon_{\text{ref}} = \tilde{\epsilon}(\mathbf{k} = 0)$. It can be shown that an equation similar to (3) can be obtained for the difference $\delta\tilde{G} = \tilde{G} - \tilde{G}_{\text{ref}}$ with respect to such reference, where the delta-like term on the right-hand side is canceled exactly. Despite this careful treatment, the evaluation of Σ is by far the heaviest part of our calculation.
- [10] R. Rinaldi *et al.*, Phys. Rev. Lett. **73**, 2899 (1994).
- [11] The GaAs/AlAs band offsets are 1.036 eV (electrons) and 0.558 eV (holes). Effective masses are 0.067 (electrons) and 0.38 (holes). Dielectric constants are 12.5 (GaAs), 10.0 (AlAs), and 2 (oxide). We neglect the variation of other band parameters between AlAs and oxide layers. Because of the exponential decay of the wave functions in the AlAs layers, these effects should be negligible when L exceeds a few nm.
- [12] This is just intended as a typical value: oxides that could be of practical relevance [see, e.g., A. Fiore *et al.*, Nature (London) **391**, 463 (1998)] have similar or smaller values. The value of the dielectric constant could be made even smaller if one could take advantage of interfaces with air [S.G. Tikhodeev *et al.*, Phys. Status Solidi (a) **164**, 179 (1997)].
- [13] Of course, there is no electron-hole asymmetry, and we could equivalently show the electron charge density and its induced polarization charge; the present choice is consistent with the choice of F_{ji}^h as "source" term, as discussed below Eq. (4).
- [14] For completeness, our calculations have been extended down to $L = 0$, although in this limit they should be taken with caution, due to the neglect of the AlAs/oxide interface effects. See also note [11].
- [15] In spite of such a dramatic enhancement, E_b is still much smaller than the GaAs band gap, so that the usual approximation which neglects the interband exchange interaction is still valid in the present structures.
- [16] This approach can be relevant also for applications to other systems, including nanocrystals embedded in glass matrices [see, e.g., A.P. Alivisatos, Science **271**, 933 (1996)] where dielectric confinement effects are expected to be strong.